

# FINITE ELEMENT-BASED OBSERVER DESIGN FOR NONLINEAR SYSTEMS WITH DELAYED MEASUREMENTS

BRANISLAV REHÁK

This paper presents a computational procedure for the design of an observer of a nonlinear system. Outputs can be delayed, however, this delay must be known and constant. The characteristic feature of the design procedure is computation of a solution of a partial differential equation. This equation is solved using the finite element method. Conditions under which existence of a solution is guaranteed are derived. These are formulated by means of theory of partial differential equations in  $L^2$ -space. Three examples demonstrate viability of this approach and provide a comparison with the solution method based on expansions into Taylor polynomials.

*Keywords:* nonlinear observer, delayed-output system, finite element method

*Classification:* 93C10, 65P99

## 1. INTRODUCTION

State feedback is a widely accepted approach to control problems in the recent control theory as well as its applications. However, in many practical cases, some states are not available to measurement; values of these states have to be reconstructed using an observer. For linear systems, one can use the Luenberger observer. Situation in nonlinear systems is more complicated, several different approaches were elaborated. First, a linear robust observer can be used, as in [24]. In this case, the nonlinearity is treated as an uncertainty. Further, let us mention the high gain observer, see e. g. [11]. It finds practical applications, see e. g. in [6] where it is used to estimate the state of a biological system. Unfortunately, this method exhibits a rather strong sensitivity to measurement noise which is a serious drawback.

Kazantsis and Kravaris in [9] developed a different approach to the observer problem for nonlinear systems. They derive an equation which can be regarded as a counterpart of the Sylvester equation proposed by Luenberger for linear systems. This equation is a linear partial differential equation (PDE) of first order with non-constant coefficients. [9] suggests to solve this equation by Taylor polynomials: right-hand side as well as coefficients are expanded into Taylor polynomials of a sufficiently high order, the solution

is also sought in form of a Taylor polynomial. To prove existence of the approximation of the solution, the Lyapunov auxiliary theorem is used. This theorem has, however, rather restrictive assumptions: all eigenvalues of the linearization of the original system around the origin must have the same sign of the real parts while purely imaginary eigenvalues are not allowed. [22] removes this restriction by introducing an iterative scheme for solution of this equation based on the iterative method originally developed for computation of stable, center-stable etc. manifolds described in [21] and successfully applied to control of practical systems in [23].

The aforementioned equation derived by [9] is closely related to the regulator equation known from the nonlinear output regulation problem. The regulator equation was numerically solved using the finite-element method (FEM) in [5, 17, 18, 19], a proof of existence of an  $L^2$  solution of this PDE on a pre-defined domain was presented in [13].

Many applications of control do not allow to obtain results of measurements immediately. Instead, the measurement process requires some time causing a time delay. This is a very common feature for instance in chemical or biological systems. Hence the need for an observer design capable of dealing with delayed measurements. There exists a large number of results, only a few of them are mentioned here.

State reconstruction if measurements are quantized is investigated in [15] together with analysis of the impact of imprecisely known value of the delay. An observer for a special case of nonlinear time delay systems – namely for polynomial systems time-delay systems - is proposed in [14]. An observer for a system with a delayed output was derived in [3] using the exact feedback linearization. This method is capable of dealing with time-varying delays in the output. The so-called cascade observer allowing to handle large time delays is proposed in [8]. A similar type of observers was also used in [10]; this paper adopts the approach of [9] to the case of systems with delayed output measurements. [4] presents a further generalization: to systems with multiple delays. A cascade observer for systems with uncertainties was proposed in the recent paper [7]. Observer design for a biological system (without delay) designed using the method analogous to the one described in this paper is presented in [12]. Let us also mention an application of nonlinear observers in biology (to the model of an artificial pancreas) shown in [2].

Application of FEM to the nonlinear observer design problem was studied in the conference paper [16]; the presented article can be considered as an expanded version. The contribution can be summarized as follows:

- An easy-to-implement method for the observer design for nonlinear systems is proposed. Both cases of delayed measurements as well as delay-free are covered.
- Existence of the nonlinear observer under less restrictive conditions than in the original papers [9, 10] is proved: the origin can be contained in the convex hull of the set of eigenvalues of the linearization of the observed system.
- A self-contained tutorial for implementation of the presented method is given to the reader.

The paper is organized as follows: the problem is defined and some results obtained in [9, 10] are repeated in the second section. Third section is devoted to the solution

in the linear case and comparison of linear and nonlinear cases. Solvability of the PDE obtained in the second section is thoroughly discussed in the fourth section, the most important result is derived here. Fifth section contains three examples, one is focused on a comparison of the proposed method with the computation procedure proposed by [9], the second one demonstrates ability of the method to deliver results under milder assumptions than those posed in [9] and, finally, the third example shows an application of the proposed approach to a practical system, moreover, sensitivity of the estimator to the mesh quality is discussed here. Numerical aspects are discussed in the sixth section. A thorough comparison with the method based on Taylor polynomials and the conclusions follow.

**Notation.**

1. The symbol  $\|\cdot\|$  denotes the vector quadratic norm.
2. If  $f : [-\tau, \infty) \rightarrow \mathbb{R}$  is a continuous function then  $\|f\|_\infty = \sup\{|f(t)|, t \in [-\tau, \infty)\}$ .
3. The time argument is sometimes omitted:  $f = f(t)$ ; the time delay can also be written in the subscript:  $f_\tau = f_\tau(t) = f(t - \tau)$ .
4. The symbol  $x$  may represent either a function  $x : \mathbb{R} \rightarrow \mathbb{R}^n$  - a solution of (1) - or a vector from  $\mathbb{R}^n$ . The meaning is clear from the context.
5. For a differentiable function  $f : \mathbb{R}^N \rightarrow \mathbb{R}$ , the symbol  $\nabla f$  is defined as  $\nabla f = (\frac{\partial f}{\partial x_1}, \dots, \frac{\partial f}{\partial x_N})^T$ .
6. If  $X$  is a square matrix, then  $\sigma(X)$  is the set of all eigenvalues of  $X$ .
7. Let  $v_1, v_2 \in \mathbb{R}^n$ ,  $v_i = (v_{i,1}, \dots, v_{i,n})^T$ ,  $i = 1, 2$ . Then  $v_1 \cdot v_2 = \sum_{j=1}^n v_{1,j} v_{2,j}$  is the inner product of vectors  $v_1$  and  $v_2$ .

2. PROBLEM SETTING

This section is based on the results of [9, 10]; these are repeated here for the sake of completeness. The plant to be observed is described by the equation (see also [4])

$$\dot{x} = F(x) \text{ for } t \geq -\tau, \quad y = h(x_\tau) \text{ for } t \geq 0 \tag{1}$$

with initial conditions

$$x(-\tau) = x_0 \in \mathbb{R}^n. \tag{2}$$

Here,  $F : \mathbb{R}^n \rightarrow \mathbb{R}^n$ ,  $h : \mathbb{R}^n \rightarrow \mathbb{R}$  are smooth functions such that  $F(0) = 0$ ,  $h(0) = 0$ . For a future purpose, it will be useful to introduce the decomposition of functions  $F$  and  $h$  as follows: let there exist matrices  $A \in \mathbb{R}^{n \times n}$ ,  $C \in \mathbb{R}^{1 \times n}$  and functions  $f : \mathbb{R}^n \rightarrow \mathbb{R}^n$   $\hat{h} : \mathbb{R}^n \rightarrow \mathbb{R}$  vanishing at the origin together with their first derivatives so that for all  $x \in \mathbb{R}^n$  holds  $F(x) = Ax + f(x)$  and  $h(x) = Cx + \hat{h}(x)$ . Then (1) can be reformulated as

$$\dot{x} = Ax + f(x), \quad y_\tau = Cx_\tau + \hat{h}(x_\tau) \tag{3}$$

where  $x(t) \in \mathbb{R}^n$ ,  $A \in \mathbb{R}^{n \times n}$ . Initial conditions are (2) again.

The following assumptions will be necessary in the subsequent text:

**Assumptions A1.**

1. The pair  $(C, A)$  is observable.
2. For any initial condition  $x_0 \in \mathbb{R}^n$ ,  $x(-\tau) = x_0$ , a unique solution  $x : \mathbb{R} \rightarrow \mathbb{R}^n$  exists.
3. The time delay  $\tau \geq 0$  is assumed to be constant and known.

**Definition** (see Kazantzis and Kravaris [9]). The observer of the system (3) is the dynamic system  $\dot{z} = \varphi(z, h(x_\tau))$ , where  $z \in \mathbb{R}^n$ ,  $\varphi : \mathbb{R}^n \times \mathbb{R} \rightarrow \mathbb{R}^n$  is a smooth function, if there exists a smooth mapping  $\Phi : \mathbb{R}^n \rightarrow \mathbb{R}^n$  such that  $\Phi(0) = 0$ , the Jacobi matrix of the function  $\Phi$  is invertible around the origin and  $z(-\tau) = \Phi(x(-\tau))$  implies  $z(t) = \Phi(x(t))$  for all  $t \geq 0$ .

In particular, we aim to find an observer defined as

$$\dot{\hat{x}} = A\hat{x} + f(\hat{x}) + L(\hat{x})(y_\tau - \hat{y}_\tau), \quad \hat{y} = h(\hat{x}). \tag{4}$$

To be specific, the goal is to find the continuous function  $L : \mathbb{R}^n \rightarrow \mathbb{R}^n$  so that the observation error  $e(t) = x(t) - \hat{x}(t)$  converges to zero for  $t \rightarrow \infty$ .

**Assumption A2.** Matrix  $\tilde{A} \in \mathbb{R}^{n \times n}$  is chosen so that all its eigenvalues are real and the following inequality holds

$$\max\{\alpha \mid \alpha \in \sigma(\tilde{A})\} < \min\left(\{0\} \cup \{\operatorname{Re} \alpha \mid \alpha \in \sigma(A)\}\right). \tag{5}$$

Using this matrix, define the following auxiliary  $n$ -dimensional system:

$$\dot{z} = \tilde{A}z + bh(x_\tau). \tag{6}$$

**Proposition 2.1.** Assume a smooth function  $\Phi : \mathbb{R}^n \rightarrow \mathbb{R}^n$  satisfies

$$\frac{\partial \Phi}{\partial x}(Ax + f(x)) = \tilde{A}\Phi(x) + bh(x_\tau). \tag{7}$$

Let  $x$  be defined by (3) and  $z$  be given by (6) with initial condition  $z(0) = \Phi(x(0))$ . Then

$$z = \Phi(x) \tag{8}$$

is valid for all  $t \geq 0$ .

*Proof.* Taking the time derivative of both sides of (8) gives

$$\dot{z} = \frac{\partial \Phi}{\partial x}(Ax + f(x))$$

which together with Eqs. (6) and (7) yields the result. □

**Assumption A3.** The pair  $(\tilde{A}, b)$  is controllable.

The following result, obtained in [9] for delay-free systems, modified in [10] for systems with delayed outputs, is repeated here for the sake of completeness.

**Proposition 2.2.** Assume that Assumptions (A1,A3) and (5) hold. Moreover, let matrix  $\frac{\partial \Phi}{\partial x}$  be invertible for all  $x \in \mathbb{R}^n$ . Then observer (4) with gain  $L$  defined by

$$L = \left( \frac{\partial \Phi}{\partial x}(\hat{x}) \right)^{-1} b \quad (9)$$

guarantees  $\lim_{t \rightarrow \infty} \|e(t)\| = 0$ .

*Proof.* Define  $z$  as in (8) and also  $\hat{z} = \Phi(\hat{x})$ . Then one has

$$\begin{aligned} & \frac{d}{dt}(z - \hat{z}) \\ &= \frac{d}{dt}(\Phi(x) - \Phi(\hat{x})) \\ &= \left( \frac{\partial}{\partial x} \Phi(x) \right) \dot{x} - \left( \frac{\partial}{\partial x} \Phi(\hat{x}) \right) \dot{\hat{x}} \\ &= \frac{\partial}{\partial x} \Phi(x) (A\Phi(x) + f(x)) - \frac{\partial}{\partial x} \Phi(\hat{x}) \left( A\Phi(\hat{x}) + f(\hat{x}) - \left( \frac{\partial \Phi}{\partial x}(\hat{x}) \right)^{-1} b (h(x_\tau) - h(\hat{x}_\tau)) \right) \\ &= \frac{\partial \Phi}{\partial x}(x) (A\Phi(x) + f(x)) - \frac{\partial \Phi}{\partial x}(\hat{x}) (A\Phi(\hat{x}) + f(\hat{x})) - bh(x_\tau) + bh(\hat{x}_\tau) \\ &= \tilde{A}\Phi(x) + bh(x_\tau) - \tilde{A}\Phi(\hat{x}) + bh(\hat{x}_\tau) - bh(x_\tau) + bh(\hat{x}_\tau) \\ &= \tilde{A}(z - \hat{z}). \end{aligned} \quad (10)$$

As  $\tilde{A}$  has all eigenvalues with negative real parts, one has  $\lim_{t \rightarrow 0} \|z - \hat{z}\| = 0$ . This relation together with invertibility of Jacobi matrix of function  $\Phi$  guarantee convergence of  $e$  to zero for  $t \rightarrow \infty$ .  $\square$

**Remark 2.3.** Invertibility of the Jacobi matrix of the function  $\Phi$  on the whole space  $\mathbb{R}^n$  is a rather strong requirement. In the following text, existence of a neighborhood of the origin where this matrix is invertible will be shown. If such an observer is implemented, it is sufficient to guarantee that the trajectory of the observer remains in this neighborhood.

### 3. PROPERTIES OF EQUATION (7) IN LINEAR AND NONLINEAR CASES

**Definition:** Let  $x_0 \in \mathbb{R}^n$ . Let  $x$  be the solution of (3) backwards in time with terminal condition  $x(0) = x_0$ . Then, define mapping  $\mathcal{T} : \mathbb{R}^n \rightarrow \mathbb{R}^n$  as  $\mathcal{T}(x_0) = x(-\tau)$ .

**Remark 3.1.** Thanks to uniqueness of the solution of (3), this map is well defined for any  $x_0 \in \mathbb{R}^n$ . Moreover, for delay-free systems,  $\mathcal{T}$  equals to identity.

If the function  $F$  is linear, the mapping  $\Phi$  can be found analytically. As this case is important for the nonlinear observer design as well, it is handled here separately. First, observe that if the plant (1) is given by

$$\dot{x} = Ax \tag{11}$$

then  $\mathcal{T}(x) = e^{-A\tau}x$  for every  $x$ .

Then, (7) attains the form

$$\bar{\Phi}A = \tilde{A}\bar{\Phi} + bCe^{-A\tau} \tag{12}$$

and the observer can be written as

$$\dot{\hat{x}} = A\hat{x} + \bar{\Phi}^{-1}b(y_\tau - \hat{y}_\tau). \tag{13}$$

Note that (12) is a Sylvester equation. As shown in [1], its solution exists if and only if the matrices  $A$  and  $\tilde{A}$  have no common eigenvalues. Matrix  $\tilde{A}$  is a design parameter, hence this condition is not restrictive. Moreover, matrix  $\bar{\Phi}$  is nonsingular, see [1] again. Observe that in the linear case, the eigenvalues of matrix  $A$  are allowed to have zero real part.

In the nonlinear case, (7) must be solved numerically. However, knowledge of the matrix  $\bar{\Phi}$  can be used to facilitate the numerical computation: assume (12) is satisfied with matrix  $\bar{\Phi}$ . Then, decompose the mapping  $\Phi$  into the linear part  $\bar{\Phi}x$  and the remaining higher-order term:

$$\Phi(x) = \bar{\Phi}x + \phi(x). \tag{14}$$

Using (14), (7) can be rewritten as

$$\left(\bar{\Phi} + \frac{\partial\phi}{\partial x}\right)(Ax + f(x)) = \tilde{A}(\bar{\Phi}x + \phi(x)) + bh(\mathcal{T}(x)). \tag{15}$$

With help of (12), (15) yields

$$\frac{\partial\phi}{\partial x}(Ax + f(x)) = \tilde{A}\phi(x) - \bar{\Phi}f(x) + bh(\mathcal{T}(x)) - bCe^{-A\tau}x. \tag{16}$$

The following proposition is a consequence of the decomposition (15).

**Proposition 3.2.** There exists a neighborhood of the origin where the Jacobi matrix  $\frac{\partial\Phi}{\partial x}(0)$  is nonsingular.

*Proof.* Eq. (14) implies

$$\frac{\partial\Phi}{\partial x}(0) = \bar{\Phi}.$$

The function  $\Phi$  is smooth, hence the result. □

To find a solution of (16), two important issues must be solved: first, mapping  $\mathcal{T}$  must be found. Next task is finding a solution of (16) based on the computed approximation of mapping  $\mathcal{T}$ .

To find an approximation of  $\mathcal{T}$ , one has to choose a sufficiently large bounded domain (open connected set)  $\Omega \subset \mathbb{R}^n$  such that  $0 \in \Omega$ . Then, a finite set  $\Omega_f \subset \Omega$  is defined so that points of  $\Omega_f$  are “well distributed” within  $\Omega$ . Subsequently, the value of the function  $\mathcal{T}$  for all points from the set  $\Omega_f$  is evaluated and, finally, an interpolation of the set  $\mathcal{T}(\Omega_f)$  is computed. This is used as an approximation of function  $\mathcal{T}$ .

**Remark 3.3.** Choice of the domain  $\Omega$  cannot be described in more detail as it depends on the specific example. This applies also to the choice of the finite set  $\Omega_f$ , hence no detailed suggestion can be given. Rather an expertise of the behavior of the algorithm gained by a couple of trials and errors would potentially lead to a satisfactory result.

#### 4. SOLUTION OF EQUATION (16)

Problem of solvability of (16) on a pre-defined domain is the problem studied of this section. Eq. (16) is linear, nonetheless, it attains a rather non-standard form: while it is a first-order equation, it differs from first-order PDEs usually met in physics, such as conservation laws. See also [22]; an equation with similar properties was solved in [13]. Prior to deriving results concerning existence of solution of (16), let us make the following assumption.

Define function  $\beta : \mathbb{R}^n \rightarrow \mathbb{R}^n$  by

$$\beta(x) = x^T A^T + f^T(x). \tag{17}$$

Let  $\phi = (\phi_1, \dots, \phi_n)^T$ . Let also symbol  $\bar{\Phi}_i$  denote the  $i$ th row of matrix  $\bar{\Phi}$ ; let also  $\mathcal{T}_i(x)$  denote the  $i$ th element of the vector  $bh(\mathcal{T}(x)) - bCe^{-\tau}x$ . Then every element of (16) can be rewritten as

$$\beta(x) \cdot \nabla \phi_i(x) - \sum_{j=1}^n \tilde{A}_{ij} \phi_j(x) = -\bar{\Phi}_i f(x) - \mathcal{T}_i(x). \tag{18}$$

Assume first matrix  $\tilde{A}$  is diagonal:  $\tilde{A}_{ii} = \text{diag}(a_1, \dots, a_n)$ . In this case, (18) implies for every  $i \in \{1, \dots, n\}$ :

$$\beta(x) \cdot \nabla \phi_i(x) - a_i \phi_i(x) = -\bar{\Phi}_i f(x) - \mathcal{T}_i(x). \tag{19}$$

This shows that all elements of the vector function  $\phi$  can be obtained by independent computation.

Conditions guaranteeing existence of a solution of (19) on a domain are presented in Lemma 1.6 in [20]. For the reader’s convenience, this lemma is repeated here as theorems dealing with existence of a solution of equations similar to (19) are not easy to find in literature. Alternatively, details can be found in Lemma II.1 in [13].

**Lemma 4.1.** Let  $\Omega \subset \mathbb{R}^n$  be a bounded domain with Lipschitz boundary,  $0 \in \Omega$ , let  $n(x)$  be the outward normal vector at the point  $x \in \partial\Omega$ . Let  $a > 0$ ,  $\beta \in (C^1(\bar{\Omega}))^n$  and  $g \in L^2(\Omega)$ .

Let  $\Gamma^- = \{x \in \partial\Omega | n(x) \cdot \beta(x) < 0\}$ . Further, assume there exists a constant  $\omega > 0$  such that

$$a - \frac{1}{2} \text{div} \beta(x) > \omega. \tag{20}$$

Then the equation

$$\beta(x) \cdot \nabla \varphi(x) + a\varphi(x) = g(x)$$

has a unique solution  $\varphi \in L^2(\Omega)$  with boundary conditions  $\varphi(x) = 0, x \in \Gamma^-$ .

**Remark 4.2.** We will see that Lemma 4.1 does not cover the case of matrix  $\tilde{A}$  having complex eigenvalues as it is applicable to scalar equations with real coefficients only. However, matrix  $\tilde{A}$  is a design parameter, therefore it can be chosen so that its eigenvalues are real.

We can now formulate conditions for existence of a solution of (19) in terms of matrices  $A, \tilde{A}$  as follows:

**Lemma 4.3.** Let the following inequality holds for every  $\tilde{a} \in \sigma(\tilde{A})$ .

$$\tilde{a} - \frac{1}{2} \text{Trace}A > 0. \tag{21}$$

Then there exists a neighborhood of the origin  $U \subset \mathbb{R}^n$  so that (20) is satisfied in  $U$ .

*Proof.* Note first that  $\text{div}\beta(x) = \text{Trace}A + \text{div}f(x)$ . Denote  $\omega = \tilde{a} - \frac{1}{2} \text{Trace}A$ . Since all derivatives of the function  $f$  are continuous and vanish at the origin, there exists a neighborhood of the origin  $U$  so that  $\|f(x)\| < \omega$  holds for all  $x \in U$ . This implies validity of (20) and thus, in turn, existence of a solution of (16) if  $\tilde{A}$  is diagonal.

Let us focus on the case when matrix  $\tilde{A}$  is not diagonal. Then, a nonsingular matrix  $T$  satisfying  $T^{-1}\tilde{A}T = J$  exists where  $J$  is the Jordan canonical form of matrix  $\tilde{A}$ . As [13] shows, this transformation changes (16) into

$$\beta(\bar{x}) \cdot \nabla_{\bar{x}} \phi_i(\bar{x}) - J\phi(\bar{x}) = \text{right hand side}. \tag{22}$$

(The symbol  $\nabla_{\bar{x}}$  denotes the  $\nabla$ -operator with derivatives with respect to the new coordinates  $\bar{x}$ .) Assume also the matrix  $J$  has  $M$  blocks on the diagonal; let their dimensions be  $n_1, \dots, n_M$ . Note that all equations containing derivatives of the functions  $\phi_{n_1}, \dots, \phi_{n_M}$  attain the same form as the equations (19). Thus they can be solved using the same procedure as described in the case of diagonal matrix  $\tilde{A}$ . Then, functions  $\phi_{n_1-1}, \dots, \phi_{n_M-1}$  are obtained by solving the equations:

$$\beta(x) \cdot \nabla \phi_{n_i-1}(x) - a_i \phi_{n_i-1}(x) - \phi_{n_i} = -\bar{\Phi}_{n_i-1} f(x) - \mathcal{T}_{n_i-1}(x), \quad i = 1, \dots, M. \tag{23}$$

This implies that function  $\phi_{n_i-1}$  can be computed with knowledge of function  $\phi_{n_i}$ . Repeating this procedure yields all functions  $\phi_i$ . □

The main result of this paper is summarized in form of the following theorem:

**Theorem 4.4.** Let Assumptions (A1,A2,A3) and (5) hold. Assume  $\Omega \subset \mathbb{R}^n, 0 \in \Omega$ , is a bounded domain such that

$$a_i - \frac{1}{2} (\text{Trace}A + \text{div}f(x)) > 0 \tag{24}$$

holds for all  $x \in \Omega$  and all  $i = 1, \dots, n$ . Assume also  $\bar{\Phi}$  solves (12). Let also  $\Gamma_i^- = \{x \in \partial\Omega | n(x) \cdot (Ax + f(x)) < 0\}$ . Then



- for every  $i \in \{1, \dots, N\}$  there exist uniquely determined functions  $\phi_i \in L^2(\Omega)$ ,  $\phi_i = 0$  on  $\Gamma_i^-$ , such that  $\phi = (\phi_1, \dots, \phi_n)^T$  solves (16).
- the observer gain  $L$  given by

$$L(\hat{x}) = \left( \bar{\Phi} + \frac{\partial \phi}{\partial x}(\hat{x}) \right)^{-1} b \quad (25)$$

is such that observer (4) guarantees  $\lim_{t \rightarrow \infty} \|e(t)\| = 0$ .

*Proof.* It is a consequence of Lemma 4.3, Theorem 4.1 and Proposition 2.2.  $\square$

**Remark 4.5.** The proof of existence of a solution of (12) is based on the Lyapunov's auxiliary theorem in [9]. Assumptions of this theorem are rather restrictive: matrix  $A$  is required to have all eigenvalues with negative real part or all its eigenvalues must have positive real part. In contrast, Theorem 4.1 yields existence of a solution of (12) under the weaker condition (21). This is the main contribution of this paper. Moreover, Theorem 1 of [9] guarantees existence of a smooth solution only locally (i. e. it implies existence of a neighborhood of the origin where the Taylor series of the solution converges, however, this neighborhood is not known; it can be too small for practical applications) while in Theorem 4.4, we have proven existence of the solution on the predefined domain  $\Omega$ .

On the other hand there is still a minor issue to be solved in the approach elaborated in this paper: Theorem 4.4 guarantees existence of a solution  $\Phi$ , however it does not imply its differentiability. This problem, called regularity of solutions of (8), is still an open issue.

**Remark 4.6.** Presence of the boundary condition on the set  $\Gamma^-$  is stipulated by the need to solve the PDE on a bounded domain, in contrast to the original formulation of (8) which is defined on the entire space  $\mathbb{R}^n$ . This boundary condition causes some error: the solution on the bounded domain  $\Omega$  with this boundary condition may differ from the restriction of the solution of (23) on the whole space  $\mathbb{R}^n$  on the domain  $\Omega$ . Fortunately, numerical experiments show that influence of these boundary conditions is significant only on a narrow region close to the border of  $\Omega$ .

The procedure can be summarized as follows:

1. Find approximation of the mapping  $\mathcal{T}$ .
2. Choose matrix  $\tilde{A}$  so that (5) holds.
3. Find the matrix  $\bar{\Phi}$ .
4. Solve (15).
5. Construct the observer gain (25).

**Remark 4.7.** Results analogous to Theorem 4.4 are usually required to prove estimates of the error caused by replacing the exact solution by an approximation obtained by the finite-element method. This paper can be regarded as a preliminary result prior to deriving these error estimates which will be the subject of a future work.

5. EXAMPLE

5.1. Example 1

The method based on the Taylor expansions, as described in [9], and the method introduced in this paper are compared here. Consider the following delay-free system:

$$\dot{x}_1 = x_2, \quad \dot{x}_2 = (-x_1 - x_1^3)e^{x_1} - 0.1x_2, \quad y = x_1.$$

Both eigenvalues of the observed system have negative real part. Consequently, the method based on Taylor expansions can be used. We choose  $b = (\frac{1}{2}, \frac{1}{2})^T$  and  $\tilde{A} = \begin{pmatrix} -1 & 0 \\ 0 & -2 \end{pmatrix}$ . Hence the Sylvester equation  $\bar{\Phi} \begin{pmatrix} 0 & 1 \\ -1 & -0.1 \end{pmatrix} = \begin{pmatrix} -1 & 0 \\ 0 & -2 \end{pmatrix} \bar{\Phi} + \begin{pmatrix} \frac{1}{2} & 0 \\ \frac{1}{2} & 0 \end{pmatrix} \begin{pmatrix} x_1 \\ x_2 \end{pmatrix}$  whose solution and, subsequently, the observer gain are

$$\bar{\Phi} = \begin{pmatrix} 0.2368 & -0.2632 \\ 0.1979 & -0.1042 \end{pmatrix}, \quad L = \begin{pmatrix} 2.9 \\ 0.71 \end{pmatrix}.$$

To obtain the approximation of the function  $\Phi$  using FEM (we will refer to this function by  $\hat{\Phi}$  in the subsequent text), software Comsol Multiphysics was used. The finite element approximation was computed on a disc with center at the origin and radius 5. This domain was divided into 13620 elements, 192 of which were boundary elements. Quadratic Lagrange elements were used. The solver provides not only values of the solution but also values of its derivatives – a significant facilitation of the implementation. These computed values were evaluated on the rectangular grid with nodes  $(x', y')$  where  $x' \in \{-1, -0.9, \dots, -0.1\} \cup \{-0.09, -0.08, \dots, 0.09\} \cup \{0.1, 0.2, \dots, 1\}$ ,  $y' \in \{-1, -0.9, \dots, -0.1\} \cup \{-0.09, -0.08, \dots, 0.09\} \cup \{0.1, 0.2, \dots, 1\}$ . Values in other points were obtained using interpolation (via the Matlab function `interp2`). The functions  $\Phi_1$  and  $\Phi_2$  are depicted in Figs. 1 and 2.

Approximation of function  $\Phi(x_1, x_2)$  by Taylor polynomials of third order was chosen. The linear terms are equal to  $\bar{\Phi} \begin{pmatrix} x_1 \\ x_2 \end{pmatrix}$ . Computation of second and third-order terms requires to find 10 coefficients. It yields

$$\tilde{\Phi}(x_1, x_2) = \begin{pmatrix} 0.2368x_1 - 0.2632x_2 - 0.1657x_1^2 + 0.0975x_1x_2 - 0.1218x_2^2 \\ -0.1590x_1^3 + 0.1383x_1^2x_2 - 0.0544x_1x_2^2 + 0.0777x_2^3 \\ 0.1979x_1 - 0.1042x_2 - 0.0391x_1^2 + 0.0260x_1x_2 - 0.0144x_2^2 \\ -0.0467x_1^3 + 0.0368x_1^2x_2 - 0.0207x_1x_2^2 + 0.0122x_2^3 \end{pmatrix}$$

and the observer gain is given by the formula (9).

Let us investigate how precisely functions  $\tilde{\Phi}$  and  $\hat{\Phi}$  approximate the function  $\Phi$ . As a measure of the precision, we take the so-called residual  $\rho$  defined as follows: if  $\Phi'$  is an approximation of the function  $\Phi$  then define  $\rho(\Phi')$  as

$$\rho(\Phi') = \frac{\partial \Phi'}{\partial x} \begin{pmatrix} x_2 \\ (-x_1 - x_1^3)e^{x_1} - 0.1x_2 \end{pmatrix} + \begin{pmatrix} 1 & 0 \\ 0 & 2 \end{pmatrix} \Phi' - \begin{pmatrix} \frac{1}{2} & 0 \\ \frac{1}{2} & 0 \end{pmatrix} \begin{pmatrix} x_1 \\ x_2 \end{pmatrix}. \quad (26)$$

Clearly, the residual of the precise solution  $\Phi$  equals identically to zero. The residual of function  $\tilde{\Phi}$  on the set  $\{(x_1, x_2) \mid |x_1| \leq 1, |x_2| \leq 1\}$  is depicted in Figs. 3 and 4.

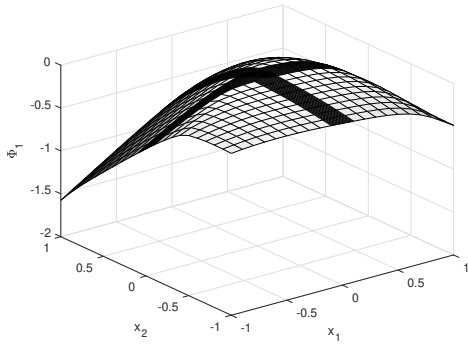


Fig. 1: Function  $\Phi_1$ .

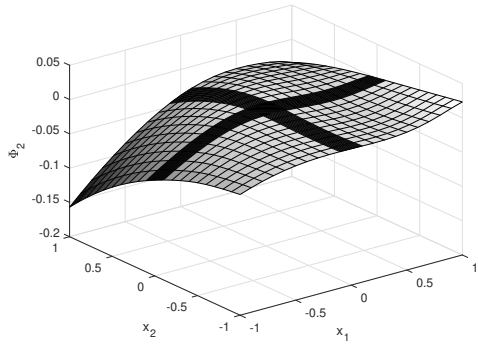


Fig. 2: Function  $\Phi_2$ .

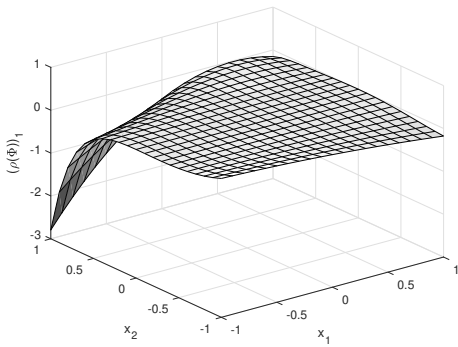


Fig. 3: Residual – first component.

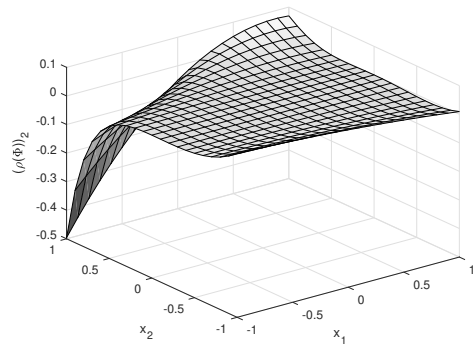


Fig. 4: Residual – second component.

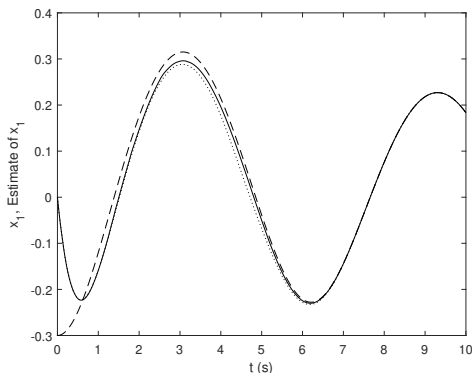


Fig. 5: State  $x_1$  and its estimate.

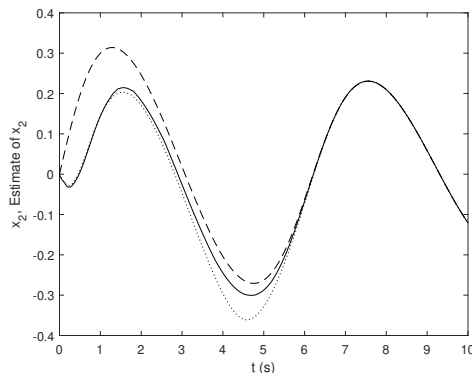


Fig. 6: State  $x_2$  and its estimate.

Note the increase of the residual with increasing distance from the origin, especially in the second quadrant. On the other hand, the residual on this disc of the function  $\widehat{\Phi}$  satisfies  $\max \|\rho(\widehat{\Phi}(x_1, x_2))\| \leq 0.2$  and is uniformly distributed over this region. Hence the approximation by the finite elements is good uniformly in this domain as opposed to the approximation by the Taylor polynomials where the approximation error increases with distance from the origin.

In the simulations, initial conditions  $(x_1(0), x_2(0)) = (-0.3, 0)$  of the plant were used while initial conditions of the observers were set to zero. Figure 5 shows convergence of the state of the FEM-based observer  $\hat{x}_1$  (solid line) to the state  $x_1$  of the observed system (represented by the dashed line). Moreover, the dotted line shows the state  $\hat{x}_1$  of the observer constructed using the third-order Taylor polynomial. Figure 6 shows convergence of non-observable state  $\hat{x}_2$  to  $x_2$ , meaning of the lines remains the same. One can see faster convergence of the observer constructed using the finite elements. Figure 7 illustrates the norm of the estimation error. The solid line shows the norm of the observation error of the FEM-based observer while the dashed line illustrates the norm of the observer computed using Taylor polynomials. Note increase of the norm of the estimation error in the time interval  $(2s, 6s)$  for the observer computed by the Taylor expansions. This increase is caused by imprecise approximation of the function  $\Phi$  by Taylor polynomials.

### 5.2. Example 2

The second example demonstrates ability of the presented method to deal with systems whose linearization exhibits purely imaginary poles. For such systems, the method proposed by [10] cannot be applied. Consider the nonlinear oscillator:

$$\dot{x}_1 = x_2, \quad \dot{x}_2 = -\sin x_1, \quad y = x_{1,\tau}$$

with the observation delay given as  $\tau = 0.2s$ .

We choose the design parameters as  $\tilde{A} = \begin{pmatrix} -1 & 0 \\ 0 & -2 \end{pmatrix}$ ,  $b = \begin{pmatrix} 1 \\ 1 \end{pmatrix}$ . For the solution of (12)

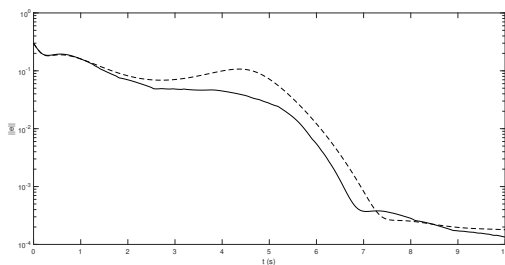


Fig. 7: Norm of the estimation error.

holds

$$\bar{\Phi} \begin{pmatrix} 0 & 1 \\ -1 & 0 \end{pmatrix} = \begin{pmatrix} -1 & 0 \\ 0 & -2 \end{pmatrix} \bar{\Phi} + \begin{pmatrix} 1 & 0 \\ 1 & 0 \end{pmatrix} \exp\left(\begin{pmatrix} 0 & -0.2 \\ 0.2 & 0 \end{pmatrix}\right), \tag{27}$$

thus, solvability conditions are satisfied. Moreover, the solution  $\bar{\Phi}$  of (27) and the observer gain for a linear observer are given by

$$\bar{\Phi} = \begin{pmatrix} 0.3907 & -0.3907 \\ 0.4714 & -0.2357 \end{pmatrix}, \quad L = \begin{pmatrix} 0.7813972 \\ 1.1787359 \end{pmatrix}.$$

Function  $\mathcal{T}(x_1, x_2)$  is approximated by third-order polynomials as

$$\mathcal{T}(x_1, x_2) = \begin{pmatrix} 0.9807x_1 - 0.1987x_2 - 0.005x_1^2 - 0.005x_1x_2 \\ +0.0335x_1^3 + 0.0269x_1^2x_2 + 0.0842x_1x_2^2 + 0.0101x_2^3 \\ 0.19867x_1 + 0.9801x_2 - 0.0004x_1^2 - 0.0002x_1x_2 + 0.0006x_2^2 \\ -0.1118x_1^3 + 0.0174x_1^2x_2 + 0.0310x_1x_2^2 - 0.0288x_2^3 \end{pmatrix}.$$

Then, (16) is solved. Its solution on the set  $\Omega = \{x \in \mathbb{R}^n \mid \|x\| \leq 2\}$ .

PDE (16) was numerically solved using FEM as described in the previous sections. Function  $\phi_1$  computed by this numerical software is shown in Figure 8.

Results of simulations can be seen in Figs. 9 and 10. Figure 9 shows the state  $x_2$  (dashed line) and its estimate (solid line). The observation error  $e$  is depicted in Figure 10. Finally, the norm of the observation error in the second component ( $\|e_2\|$ ) is shown in Figure 11 (solid line). The dashed line in this figure represents the norm of the second component of the observation error if a linear observer (with observer gain equal to  $\bar{\Phi}^{-1}b$ ). One can see faster convergence of the nonlinear observer.

### 5.3. Example 3

The plant considered in this example is a magnetic levitation system described in [23]. The system is described by equations

$$\dot{x} = v, \quad \dot{v} = g - \frac{C}{m} \frac{u + u_0}{(x + x_0 + d)^2}, \tag{28}$$

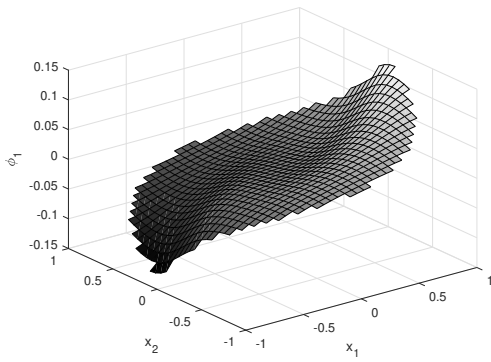


Fig. 8: Function  $\phi_1$ .

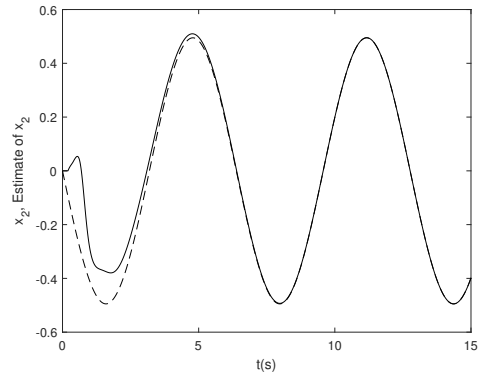


Fig. 9: State  $x_2$  and its estimate.

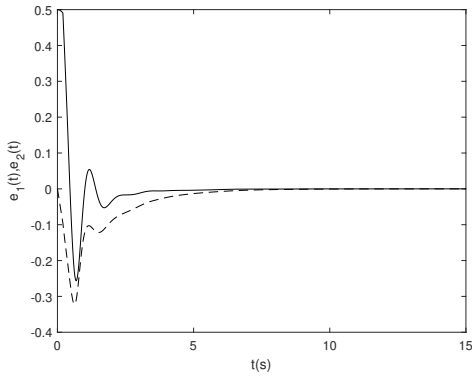


Fig. 10: Observation error.

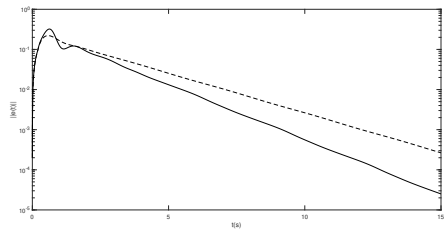


Fig. 11: Norm of the observation error.

where  $x$  is the vertical position of the ball to be levitated,  $v$  is its velocity. The meaning of the parameters is as follows:  $g = 9.81ms^{-2}$  is the gravitational constant,  $C = 1.2281 \times 10^{-4}Nm^2A^{-2}$  is the electromagnetic constant,  $m = 0.0661kg$  is the mass of the ball,  $d = 0.00571m$  is the parameter of the actuator. The ball should be stabilized in the equilibrium position  $x_0 = 0.007m$ ;  $u_0 = \sqrt{\frac{mg}{C}}(x_0 + d)$  is the control signal corresponding to this equilibrium position of the ball.

Using the transformation  $x_1 = x - x_0$ ,  $x_2 = v$ , one can rewrite (28) as

$$\dot{x}_1 = x_2, \quad \dot{x}_2 = g\left(1 - \frac{(x_0 + d)^2}{(x_1 + x_0 + d)^2}\right) - \frac{C}{m(x_1 + x_0 + d)^2}u. \tag{29}$$

In accordance with [23], the system is controlled by the control law  $u = -268.46x_1 - 6.8332x_2$ . This is the result of the LQ control design (for the linearization of (29)) with weighting matrices  $Q = \begin{pmatrix} 1 & 0 \\ 0 & 1 \end{pmatrix}$ ,  $R = 1000$ .

The observer is designed with  $C = (1, 0)$  which corresponds to the practical setting (no velocity measurement is available). Moreover, we choose  $b = (1, 1)^T$  and  $\tilde{A} = \begin{pmatrix} -50 & 0 \\ 0 & -51 \end{pmatrix}$ . Then, the observer is faster than the fastest mode of the plant.

Solution of (12) yields

$$\bar{\Phi} = \begin{pmatrix} 0.052276 & -0.0010455 \\ 0.048229 & -0.000945667 \end{pmatrix}.$$

The function  $\phi$  was computed using FEM on the elliptical domain  $\Omega = \{(x_1, x_2) \mid (\frac{x_1}{0.005})^2 + (\frac{x_2}{0.02})^2 \leq 1\}$ . Function  $\Phi(x_1, x_2)$  was approximated by a polynomial of second degree.

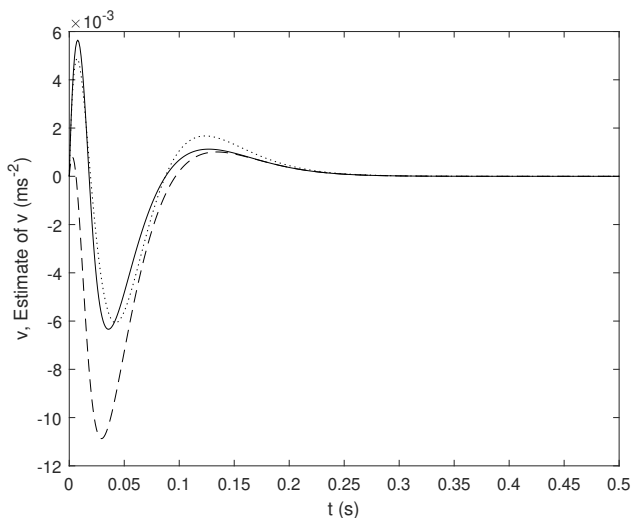


Fig. 12: Estimate of the velocity of the ball.

Figure 12 illustrates the behavior of the controlled system where the controller computes the control action from the values provided by the observer with initial conditions

Mesh number	1	2	3
$N_p$	172	725	3789
$N_{el}$	294	1352	7384
$N_{dof}$	1274	5602	29922

Tab. 1: Mesh parameters.

$x_1(0) = 4 * 10^{-4}m$ ,  $x_2(0) = 0$ . The dashed line is the velocity of the ball of the observed plant, the solid line represents its estimate computed by the nonlinear observer. For comparison, dotted line shows the estimate of the velocity given by the linear observer.

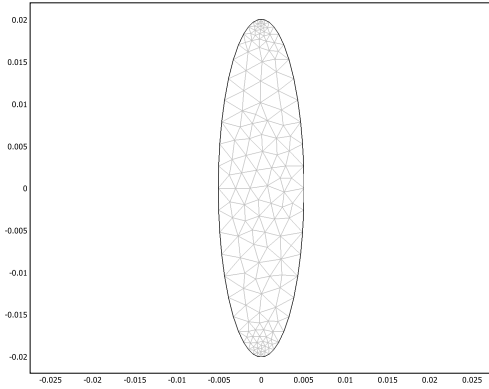
To apply the observer successfully in the control loop, the observation must be faster than any mode of the observed system. This is why the eigenvalues of matrix  $\tilde{A}$  have rather large absolute value. Unfortunately, this fact reflects in a strong sensitivity of the computed solution on computational errors, including also a strong influence of the mesh quality on the result. Figs. 13a-13c show three different meshes on the domain  $\Omega$  defined above. The mesh parameters are given in Table 1. The meaning of the columns is as follows:  $N_p$ : number of nodes,  $N_{el}$ : number of elements,  $N_{dof}$ : the total number of degrees of freedom of this discretization. The mesh depicted in Figure 13c was used for computations above. Let us note that the mesh generator contained in Comsol Multiphysics software with standard settings generated the mesh in Figure 13a. The following mesh was created by refining this mesh uniformly and manually in an area around the origin. Finally, further refinement around the origin gives the mesh 13c.

Function  $\phi$  was evaluated numerically on these meshes. Results of these computations were used to construct three observers whose behavior is illustrated in Figure 14. The dotted line stands for the variable  $x_2$  of the original system, dashed line represents the estimate delivered by the first mesh, dash-dot line is used to illustrate the estimate from the second mesh and finally, the third mesh gives the estimate depicted by the solid line. One can see the results delivered by the first mesh are grossly inaccurate (significantly worse than those obtained from a linear observer) but the second mesh yields results comparable with the third mesh.

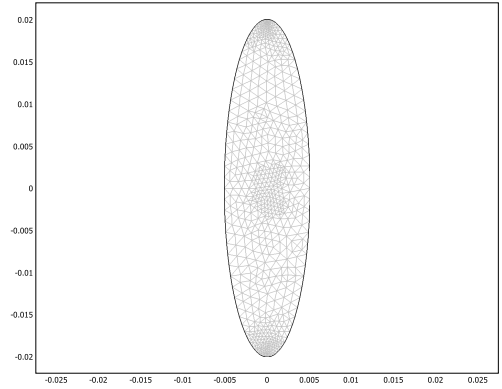
## 6. COMPARISON WITH THE METHOD BASED ON TAYLOR EXPANSIONS

Paper [10] (and, in the delay-free case, [9]) use expansions to Taylor polynomials to find the solution of (7). The right-hand side as well as the function  $f$  are approximated by their Taylor polynomials, the solution is sought also in form of a Taylor polynomial which is probably the most widely used method for solution of PDEs of this type. Although this method is easy to explain and understand, it suffers from some drawbacks. First, the result is only “local”, convergence is guaranteed in general only in an unknown neighborhood of the origin. Moreover, precision of the approximation decreases with distance from the origin. In contrast, the approach presented here gives results whose precision on an a-priori given set (the set  $\Omega$ ) is guaranteed by the FEM solver. One can also note that computation of the Taylor polynomials requires lengthy calculations, even for the third-order polynomials. The results are difficult to obtain without help of a symbolic software.

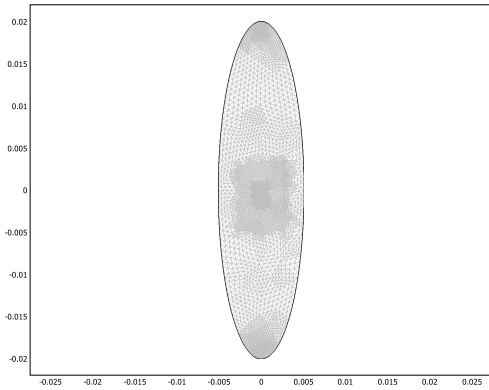




(a) Mesh 1.



(b) Mesh 2.



(c) Mesh 3.

Fig. 13

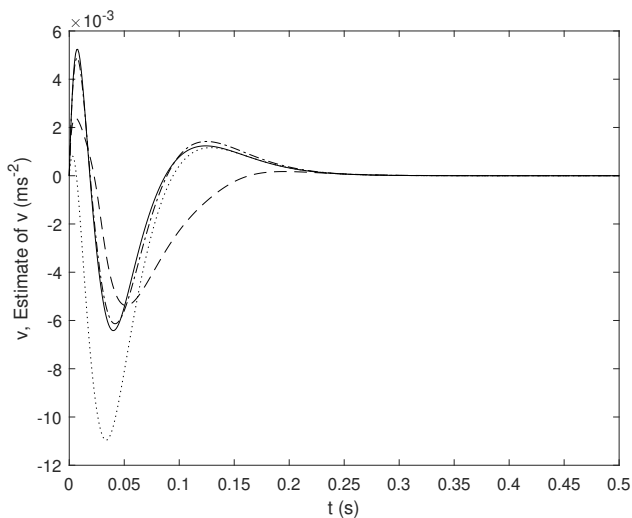


Fig. 14: Estimation of the ball velocity using different meshes.

The design method based on finite elements is quite straightforward, however, its application requires some knowledge of numerical solution of PDEs. The crucial point seems to be a fine mesh in the region where the PDE (16) is solved. While a coarse mesh might produce a quite precise approximation the function  $\Phi$ , its derivatives are approximated with insufficient precision. The fact that a matrix which is inverted is built up of these derivatives emphasizes the need for a good approximation of these derivatives.

### 7. CONCLUSIONS

A FEM-based numerical design of a nonlinear observer with delayed measurements was presented. Existence of a solution of the equations involved in the design process were discussed, conditions of convergence of the method were derived. Viability of the method was illustrated by an example.

In future, the problem of existence of invertibility of the Jacobi matrix of the function  $\Phi$  on a pre-defined domain will be studied. Also, estimates of the error between the numerical and exact solution of the PDE will be derived.

### ACKNOWLEDGEMENTS

This work was supported by the Czech Science Foundation through the Grant No. GA19-07635S.

## REFERENCES

- 
- [1] G. Birkhoff and S.M. Lane: A Survey of Modern Algebra. CRC Press, 2017. DOI:10.1201/9781315275499
  - [2] A. Borri, F. Cacace, A. De Gaetano, A. Germani, C. Manes, P. Palumbo, S. Panunzi, and P. Pepe: Luenberger-like observers for nonlinear time-delay systems with application to the artificial pancreas: The attainment of good performance. *IEEE Control Syst.* *37* (2017), 4, 33–49. DOI:10.1109/mcs.2017.2696759
  - [3] F. Cacace, A. Germani, and C. Manes: An observer for a class of nonlinear systems with time varying observation delay. *Systems Control Lett.* *59* (2010), 305–312. DOI:10.1016/j.sysconle.2010.03.005
  - [4] F. Cacace, A. Germani, and C. Manes: A chain observer for nonlinear systems with multiple time-varying measurement delays. *SIAM J. Control Optim.* *52* (2014), 1862–1885. DOI:10.1137/120876472
  - [5] S. Čelikovský and B. Rehák: Output regulation problem with nonhyperbolic zero dynamics: Femlab-based approach. *IFAC Proc. Vol. 37* (2004), 21, 651–656. 2nd IFAC Symposium on System Structure and Control, Oaxaca 2004. DOI:10.1016/s1474-6670(17)30544-x
  - [6] S. Čelikovský, J. A. Torres-Munoz, and A. Dominguez-Bocanegra: Adaptive high gain observer extension and its application to bioprocess monitoring. *Kybernetika* *54* (2018), 1, 155–174. DOI:10.14736/kyb-2018-1-0155
  - [7] M. Farza, O. Hernández-González, T. Ménard, B. Targui, M. M’Saad, and C.-M. Astorga-Zaragoza: Cascade observer design for a class of uncertain nonlinear systems with delayed outputs. *Automatica* *89* (2018), 125–134. DOI:10.1016/j.automatica.2017.12.012
  - [8] A. Germani, C. Manes, and P. Pepe: A new approach to state observation of nonlinear systems with delayed output. *IEEE Trans. Automat Control* *47* /2002), 1, 96–101.
  - [9] N. Kazantzis and C. Kravaris: Nonlinear observer design using Lyapunov’s auxiliary theorem. *Systems Control Lett.* *34* (1998), 241–247. DOI:10.1016/s0167-6911(98)00017-6
  - [10] N. Kazantzis and R. Wright: Nonlinear observer design in the presence of delayed output measurements. *Systems Control Lett.* *54* (2005), 877–886. DOI:10.1016/j.sysconle.2004.12.005
  - [11] H. Khalil: *Nonlinear Systems*. Prentice Hall, New Jersey 2001.
  - [12] V. Lynnyk and B. Rehák: Design of a nonlinear observer using the finite element method with application to a biological system. *Cybernet. Physics* *8* (2019), 292–297. DOI:10.35470/2226-4116-2019-8-4-292-297
  - [13] B. Rehák: Alternative method of solution of the regulator equation: L2 -space approach. *Asian J. Control* *14* (2011), 1150–1154. DOI:10.1002/asjc.416
  - [14] B. Rehák: Sum-of-squares based observer design for polynomial systems with a known fixed time delay. *Kybernetika* *51* (2015), 856–873. DOI:10.14736/kyb-2015-5-0856
  - [15] B. Rehák: Observer design for a time delay system via the Razumikhin approach. *Asian J. Control* *19* (2017), 6, 2226–2231. DOI:10.1002/asjc.1507
  - [16] B. Rehák: Finite-element based observer design for nonlinear systems with delayed measurements. *IFAC-PapersOnLine* *51* (2018), 14, 201–206. 14th IFAC Workshop on Time Delay Systems TDS 2018. DOI:10.1016/j.ifacol.2018.07.223

- [17] B. Reháč, J. Orozco-Mora, S. Čelikovský, and J. Ruiz-León: Real-time error-feedback output regulation of nonhyperbolically nonminimum phase system. In: 2007 American Control Conference 2007, pp. 3789–3794. DOI:10.1109/acc.2007.4282643
- [18] B. Reháč and S. Čelikovský: Numerical method for the solution of the regulator equation with application to nonlinear tracking. *Automatica* 44 (2008), 5, 1358–1365. DOI:10.1016/j.automatica.2007.10.015
- [19] B. Reháč, S. Čelikovský, J. Ruiz-León, and J. Orozco-Mora: A comparison of two Fem-based methods for the solution of the nonlinear output regulation problem. *Kybernetika* 45 (2009), 427–444.
- [20] H.-G. Roos, M. Stynes, and L. Tobiska: Numerical Methods for Singularly Perturbed Differential Equations. Springer, Berlin 1996. DOI:10.1007/978-3-662-03206-0
- [21] N. Sakamoto and B. Reháč: Iterative methods to compute center and center-stable manifolds with application to the optimal output regulation problem. In: Proc. 50th IEEE Conference on Decision and Control and European Control Conference (CDC-ECC), Orlando 2011. DOI:10.1109/cdc.2011.6161089
- [22] N. Sakamoto, B. Reháč, and K. Ueno: Nonlinear Luenberger observer design via invariant manifold computation. In: Proc. 19th IFAC World Congress, 2014, Cape Town 2014. DOI:10.3182/20140824-6-za-1003.01103
- [23] A. T. Tran, S. Suzuki, and N. Sakamoto: Nonlinear optimal control design considering a class of system constraints with validation on a magnetic levitation system. *IEEE Control Systems Lett.* 1 (2017), 2, 418–423. DOI:10.1109/lcsys.2017.2717932
- [24] Y. Yu and Y. Shen: Robust sampled-data observer design for Lipschitz nonlinear systems. *Kybernetika* 54 (2018), 4, 699–717. DOI:10.14736/kyb-2018-4-0699

*Branislav Reháč, The Czech Academy of Sciences, Institute of Information Theory and Automation, Pod Vodárenskou věží 4, 182 08 Praha 8. Czech Republic.  
e-mail: rehacb@utia.cas.cz*